

High-Resolution Infrared Synchrotron Investigation of (HCN)₂ and a Semi-Experimental Determination of the Dissociation Energy D_0

D. Mihrin,^[a] P. W. Jakobsen,^[a] A. Voute,^[a] L. Manceron,^[b, c] and R. Wugt Larsen^{*[a]}

The high-resolution infrared absorption spectrum of the donor bending fundamental band ν_6^1 of the homodimer (HCN)₂ has been collected by long-path static gas-phase Fourier transform spectroscopy at 207 K employing the highly brilliant 2.75 GeV electron storage ring source at Synchrotron SOLEIL. The rovibrational structure of the ν_6^1 transition has the typical appearance of a perpendicular type band associated with a Σ - Π transition for a linear polyatomic molecule. The total number of 100 assigned transitions are fitted employing a standard semi-rigid linear molecule Hamiltonian, providing the band origin ν_0 of 779.05182(50) cm⁻¹ together with spectroscopic parameters for the degenerate excited state. This band origin, blue-shifted by 67.15 cm⁻¹ relative to the HCN monomer, provides the final

significant contribution to the change of *intra*-molecular vibrational zero-point energy upon HCN dimerization. The combination with the vibrational zero-point energy contribution determined recently for the class of large-amplitude *inter*-molecular fundamental transitions then enables a complete determination of the total change of vibrational zero-point energy of 3.35 ± 0.30 kJ mol⁻¹. The new spectroscopic findings together with previously reported benchmark CCSDT(Q)/CBS electronic energies [Hoobler *et al.* *ChemPhysChem.* **19**, 3257–3265 (2018)] provide the best semi-experimental estimate of 16.48 ± 0.30 kJ mol⁻¹ for the dissociation energy D_0 of this prototypical homodimer.

1. Introduction

A highly accurate experimental determination of the dissociation energy D_0 for a binary non-covalent weakly bound cluster molecule is notoriously challenging and has solely been demonstrated for a small number of molecular systems. In the elementary case of the simple hydrogen-bonded (HF)₂ homodimer, direct measurements of unparallel accuracy based on state-to-state vibrational pre-dissociation dynamics by Miller *et al.*^[1] provided a D_0 -value of 1062 ± 1 cm⁻¹. In a fully non-empirical quantum chemical computational work, Hobza *et al.*^[2] employed large basis set CCSD(T) calculations including contributions of higher excitations up to the full CCSDTQ level and relativistic and diagonal Born-Oppenheimer corrections together with anharmonic vibrational zero-point energies in order to reproduce the dissociation energy. This demanding computational approach solely available for molecular systems of a very

limited size, however, still underestimated the experimental dissociation energy by 25 cm⁻¹ owing to the inaccuracy of the second order vibrational perturbation theory approach employed to predict the vibrational zero-point energy of the (HF)₂ system. In a similar direct fragment analysis based on velocity map imaging and resonance-enhanced multiphoton ionization, Rocher-Casterline *et al.* provided an accurate experimental dissociation energy of 1105 ± 10 cm⁻¹ for the slightly larger prototypical hydrogen-bonded (H₂O)₂ homodimer.^[3] This experimental determination helped to validate the accuracy of different theoretical methodologies and most notably the comprehensive work by Shank *et al.* who constructed an intermolecular potential energy surface (IPES) based on 30 000 *ab initio* CCSD(T) grid points.^[4] This full-dimensional IPES was fitted to reproduce available benchmark calculations of the interaction energy D_e ^[5] and employed for diffusion Monte Carlo calculations of the vibrational zero-point energy of (H₂O)₂ to predict a dissociation energy D_0 of 1103 cm⁻¹. An alternative indirect approach was demonstrated by Kollipost *et al.*^[6] for an even larger system, the doubly hydrogen-bonded dimer of formic acid (HCOOH)₂, based on the macroscopic dissociation equilibrium constant and the rich rovibrational spectroscopic datasets available for this strongly bound system. After an extensive far-infrared jet spectroscopic characterization of large-amplitude hydrogen bond vibrational modes,^[6,7] the combination of room temperature dissociation equilibrium constants and statistical treatments of the rovibrational partition function involving the complete set of altogether 24 vibrational fundamental transitions enabled the determination of an experimental D_0 -value of 59.5(5) kJ mol⁻¹. The present work demonstrates an indirect semi-experimental strategy for the

[a] D. Mihrin, Dr. P. W. Jakobsen, A. Voute, Prof. R. Wugt Larsen
Department of Chemistry, Technical University of Denmark
Kemitorvet 206, 2800 Kgs. Lyngby, Denmark
E-mail: rew@kemi.dtu.dk

[b] Dr. L. Manceron
Synchrotron SOLEIL, L'Orme des Merisiers
Saint-Aubin-BP 48, 91192 Gif-sur-Yvette Cedex, France

[c] Dr. L. Manceron
Lab. MONARIS, CNRS-UPMC UMR8233
4 Place Jussieu, 75230 Paris Cedex, France

Supporting information for this article is available on the WWW under <https://doi.org/10.1002/cphc.201900811>

© 2019 The Authors. Published by Wiley-VCH Verlag GmbH & Co. KGaA.
This is an open access article under the terms of the Creative Commons Attribution License, which permits use, distribution and reproduction in any medium, provided the original work is properly cited.

homodimer of HCN, where an extensive rovibrational dataset for the basically complete set of thirteen fundamental transitions is now available.

The initial spectroscopic investigations of $(\text{HCN})_2$ by microwave molecular beam spectroscopy established the linear CH \cdots N hydrogen bond configuration in the vibrational ground state.^[8,9,11–17] Subsequently, complementary high-resolution infrared^[18–24] and Raman^[25,26] spectroscopic studies employing a combination of static cryogenic long-path absorption cells and supersonic jet expansions have provided accurate hydrogen bond induced spectral shifts and (partly) resolved the rovibrational structures of the more or less perturbed intramolecular CH (ν_1 and ν_2) and CN (ν_3 and ν_4) stretching bands of both the hydrogen bond donor and acceptor moieties. The dedicated line shape analysis and extracted line width parameters from the high-resolution infrared spectra of the hydrogen bond acceptor and donor CH stretching bands have provided crucial information about pre-dissociation lifetimes and indirectly the coupling between these intramolecular vibrational modes and the large-amplitude intermolecular hydrogen bond modes of $(\text{HCN})_2$.^[18,19,23] Miller *et al.*^[20] generated optothermal sub-Doppler resolution (near)-infrared spectra of the $\nu_1 + \nu_9' - \nu_9''$ hot band and the $\nu_1 + \nu_9'$ sum band providing indirect information about the doubly degenerate ν_9' fundamental transition associated with the intermolecular large-amplitude hydrogen bond acceptor librational motion. This ν_9' band origin was subsequently detected directly at $40.7518711(67) \text{ cm}^{-1}$ by a tunable far-infrared Stark spectroscopy investigation.^[27] The observed reduction of the electric dipole moment of $0.54(5) \text{ D}$ in the excited state relative to the ground-state value of $6.023(31) \text{ D}$ demonstrated a highly anharmonic nature of this vibrational normal coordinate. The large-amplitude vibrational motion involving intermolecular hydrogen bonds is in general found to be highly anharmonic in nature and challenging for *ab initio* methodologies.^[28–32] The second fundamental transition associated with the class of large-amplitude anharmonic intermolecular vibrational modes, the hindered translational motion involving both HCN subunits or intermolecular stretching ν_5 , has been observed indirectly at ca. 101 cm^{-1} from vibrational satellites in the microwave region^[8]. Recently, the final fundamental transition associated with this class of motion, the doubly degenerate intermolecular large-amplitude hydrogen bond donor librational mode ν_8' has been observed at $119.11526(60) \text{ cm}^{-1}$ by the present authors^[33] employing a high-resolution long-path Fourier transform THz spectroscopy approach involving highly brilliant synchrotron radiation.^[34–37] These experimental rovibrational observations would help to validate or even construct a future (semi-experimental) full-dimensional IPES for this prototypical $(\text{HCN})_2$ system. In the present work we extend this long-path synchrotron spectroscopy approach to explore the region above 700 cm^{-1} , where the two until now non-observed vibrational fundamental transitions for $(\text{HCN})_2$ associated with the doubly degenerate donor (ν_6') and acceptor (ν_7') bending modes were expected. In contrast to the acceptor bending fundamental, the donor bending fundamental has been predicted to be significantly blue-shifted relative to the HCN monomer fundamental at

711.90 cm^{-1} in the order of 55 to 85 cm^{-1} by harmonic^[33] and anharmonic force field calculations^[38], respectively. This doubly degenerate ν_6' transition then alone contribute with ~ 0.65 – 1.0 kJ mol^{-1} to the total change of vibrational zero-point energy. A recent fully non-empirical quantum chemical computational work by Hoobler *et al.*^[38] has provided an AE-CCSDT(Q)/CBS benchmark value including relativistic and diagonal Born-Oppenheimer corrections for the interaction energy D_e of $19.83 \text{ kJ mol}^{-1}$. Instead of employing Hoobler *et al.*'s theoretical anharmonic vibrational zero-point energy for $(\text{HCN})_2$ based on second order vibrational perturbation theory, we are now able to estimate a semi-experimental value of this important quantity and reach an accurate dissociation energy D_0 .

Experimental

HCN was synthesized by dropwise addition of concentrated H_2SO_4 (99.999%, Sigma Aldrich) onto KCN ($\geq 98.0\%$, Sigma Aldrich) *in vacuo* with immediate condensation of the evolved gas. Minor impurities of CO, CO_2 and $(\text{CN})_2$ were subsequently removed by several freeze-pump-thaw cycling procedures. A sublimation pressure of 1.7 hPa HCN resided in a static long-path cryogenic absorption cell at a PID regulated cell body temperature of $207 \pm 0.2 \text{ K}$.^[39] The multipass arrangement of the long-path absorption cell is based on the optical design by Chernin and Barskaya^[40] and provided a total optical path length of 105 m . A specialized transfer optics design is employed to extract and refocus the probe beam onto the sample compartment of a Bruker IFS 125 HR Fourier transform spectrometer (FTS) located at the far-infrared AILES beam-line at Synchrotron SOLEIL as described elsewhere.^[39] High brightness broadband synchrotron radiation from the third generation 2.75 GeV electron storage ring providing a ring current of 450 mA was focused onto the aperture of the FTS, providing a signal-to-noise gain at high spectral resolution relative to a conventional thermal radiation source.^[41] A total number of 1408 sample single-beam interferograms, corresponding to a total scan time of 34 hours, was collected employing a Ge on KBr beam splitter and a highly sensitive home-built liquid helium cooled HgCdTe detector mounted with a cold 940 cm^{-1} low-pass filter.^[42] The recorded sample interferograms were Fourier transformed employing Mertz phase correction and boxcar apodization. A sample spectral resolution of 0.004 cm^{-1} was selected as the best compromise between the resulting signal-to-noise and the separation of observed spectral features. The background single-beam spectra were collected at a lower but still sufficient spectral resolution to capture the dominant interference fringes. The absolute wavenumber scale of the resulting infrared absorption spectra was calibrated against the accurate CO_2 line positions reported by Horneman.^[43] The precision of the observed line positions is estimated to be better than 0.002 cm^{-1} .

2. Rovibrational Spectral Analysis

The collected infrared average absorbance spectrum is dominated by the strong degenerate bending fundamental of the HCN monomer in the entire range from 525 cm^{-1} to 835 cm^{-1} . The R-branch of this band therefore gives rise to a series of strong rovibrational lines with a spacing around 2.9 cm^{-1} in the spectral window above the HCN monomer band origin of 711.9 cm^{-1} , where both the acceptor bending transition ν_7' and

the donor bending transition ν_6^1 of $(\text{HCN})_2$ are expected. The collected absorbance spectrum does not show any sign of the slightly perturbed ν_7^1 transition of $(\text{HCN})_2$ due to the very saturated HCN monomer absorptions in the vicinity of the band origin. However, a distinct Q-branch structure is clearly observed around 779.05 cm^{-1} in the gap between two strong HCN monomer lines. The Q-branch degrades towards lower energies indicating a negative value of $\Delta B = (B' - B'')$ and is accompanied by weaker R- and P-branches. An extensive series of more than 35 lines with a spacing around 0.10 cm^{-1} in the range between 781.4 cm^{-1} and 785.4 cm^{-1} belonging to the R-branch is readily observable, whereas the corresponding P-branch is severely overlapped by a second weaker Q-branch at 777.2 cm^{-1} (not shown), which we tentatively assign to a hot band transition originating from the populated ν_9^1 level. The observed rovibrational structure thus has the typical appearance of a perpendicular type band of a Σ - Π transition for a linear polyatomic molecule. Figure 1 shows the observed spectrum in the narrow region of this Q-branch, blue-shifted by 67.15 cm^{-1} relative to the HCN monomer fundamental, which is consequently assigned to the significantly perturbed ν_6^1 transition.

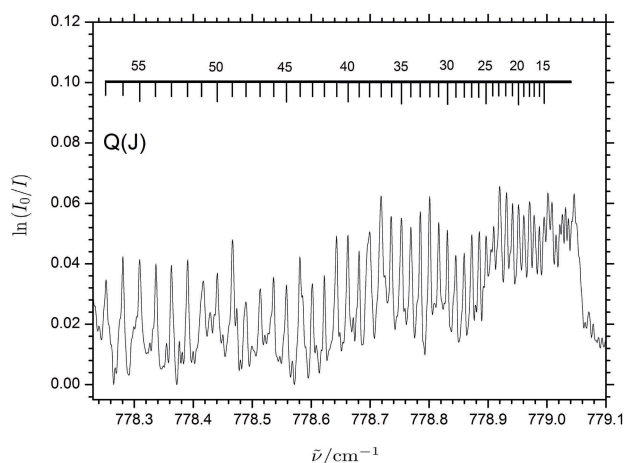


Figure 1. Portion of the infrared absorbance spectrum of the homodimer $(\text{HCN})_2$ showing the ν_6^1 band in the spectral region of the central Q-branch. The numbered lines above the trace indicate the assigned J -values for the individual rovibrational transitions (see the electronic supplemental material).

The observed rotational structure of the band was analyzed employing a standard semi-rigid polyatomic linear molecule Hamiltonian as implemented in the PGOPHER software package developed by Western^[44]. This semi-rigid linear molecule Hamiltonian is based on the rovibrational energy expressions for the vibrational ground state E'' and the vibrational excited state E' given in eqs. (1) and (2) including the rotational constants B'' and B' , the quartic centrifugal distortion constants D''_J and D'_J , together with the l -type doubling constant q for the degenerate level associated with the ν_6^1 transition.

$$E'' = B''J(J+1) - D''_J J^2(J+1)^2 \quad (1)$$

$$E' = B'J(J+1) - D'_J J^2(J+1)^2 \pm \frac{1}{2}qJ(J+1) \quad (2)$$

The P- and R-branch transitions occur to the lower components of the doublets with an effective rotational constant ($B' - \frac{1}{2}q$) according to the general symmetry selection rule, whereas the Q-branch transitions occur to the upper components of the doublets with an effective rotational constant ($B' + \frac{1}{2}q$). Separate rovibrational analyses of the Q-branch and the P-, R-branch system are therefore required for the determination of B' and q . The values of the ground-state constants B'' and D''_J , were constrained to the values reported by Larsen *et al.*^[24], based on the most comprehensive rovibrational analysis available in the literature for $(\text{HCN})_2$.

Several J -assignments of the Q-branch transitions were tested both with and without the incorporation of the l -type doubling parameter. The specific assignment of the Q-branch transitions shown in Figure 1 resulted in a significantly smaller fitting residual relative to other proposed assignments. The correct J -assignments of the R-branch transitions were rather straightforward as the unresolved beginning of the strong Q-branch clearly indicates the origin of the band (Figure 1). A total number of 100 observed P- ($34 \leq J'' \leq 45$), Q- ($13 \leq J'' \leq 63$) and R-transitions ($20 \leq J'' \leq 63$) were subsequently fitted simultaneously employing the Hamiltonian including the l -type doubling constant and the resulting spectroscopic constants are given in Table 1. The obtained fitting residual of 0.00154 cm^{-1} is more than three times smaller than the spectral resolution as expected^[10] and the observed and calculated rovibrational transition energies are provided in the electronic supporting information.

3. A Semi-Experimental Vibrational Zero-Point Energy and Dissociation Energy D_0

The present observed ν_6^1 fundamental band origin provides the final significant contribution to the change of *intra*-molecular vibrational zero-point energy upon HCN dimerization denoted $\Delta\text{ZPE}_{\text{intra}}$ as the only non-observed *intra*-molecular vibrational fundamental transition missing is associated with the acceptor

Table 1. The spectroscopic constants (cm^{-1}) and resulting fitting parameters obtained from the rovibrational analysis of the observed donor bending fundamental band ν_6^1 of $(\text{HCN})_2$.^[a]

ν_0	779.05182(50)
B'	0.05803055(58)
D'_J	$8.151(14) \cdot 10^{-8}$
q	$1.424(50) \cdot 10^{-5}$
$N^{[b]}$	100
$\sigma^{[c]}$	0.00154

^[a] The ground-state constants were constrained to $B'' = 0.0582570 \text{ cm}^{-1}$ and $D''_J = 7.745 \cdot 10^{-8} \text{ cm}^{-1}$.^[23] ^[b] Number of observations. ^[c] Residual of fit.

Table 2. The observed (anharmonic) and harmonic CCSD(T)-F12b/aug-cc-pVQZ vibrational fundamental energies (cm⁻¹) for the linear (HCN)₂ homodimer classified according to the irreducible representations of the point group C_{∞v} with corresponding vibrational normal mode descriptions.

	ν_{obs}	$\omega_{CCSD(T)-F12b}^{(f)}$	Symmetry Species	Mode Description
ν_1	3308.3175(5) ^[a]	3435.0	Σ_g	Acceptor CH Stretch
ν_2	3241.5588(30) ^[a]	3356.5	Σ_g	Donor CH Stretch
ν_3	2104.6(3) ^[b]	2142.1	Σ_g	Acceptor CN Stretch
ν_4	2094.7(3) ^[b]	2120.8	Σ_g	Donor CN Stretch
ν_5	101 ^[c]	118.8	Σ_g	N ···HC Stretch
ν_6^1	779.05182(50) ^[d]	814.2	Π	Donor HCN Bend
ν_7^1	723(2) ^[e]	739.8	Π	Acceptor HCN Bend
ν_8^1	119.11526(60) ^[f]	137.2	Π	Donor Libration
ν_9^1	40.7518711(67) ^[g]	48.0	Π	Acceptor Libration

^[a] Jucks *et al.*^[18] ^[b] Maroncelli *et al.*^[24,25] ^[c] Georgiou *et al.*^[13] ^[d] Present work. ^[e] Anharmonic prediction by Hoobler *et al.*^[37] (see text). ^[f] Mihrin *et al.*^[32] ^[g] Grushow *et al.*^[26]

bending mode ν_7^1 , which according to quantum chemical predictions is just slightly perturbed relative to the isolated HCN monomer bending band origin.^[33,38] In the discussion of how to make a reliable estimate of the total change of vibrational zero-point energy upon dimerization $\Delta ZPE_{total} = \Delta ZPE_{intra} + \Delta ZPE_{inter}$, where the term ΔZPE_{inter} denotes the contribution from the class of large-amplitude *inter*-molecular vibrational modes, we will first address the usual vibrational term values $G(\nu)$ given by the second order perturbation theory expression below. For simplicity, we consider the standard vibrational term expression formulated for an asymmetric top molecule although some of these terms will be identical for a polyatomic linear molecular system as (HCN)₂:

$$G(\nu) = \sum_r \omega_r \left(\nu_r + \frac{1}{2} \right) + \sum_{r>s} x_{rs} \left(\nu_r + \frac{1}{2} \right) \left(\nu_s + \frac{1}{2} \right) \quad (3)$$

including the r -th harmonic vibrational energy ω_r , the vibrational anharmonicity constants x_{rs} and the vibrational quantum number ν_r for the normal coordinate r . The “true” vibrational zero-point energy $G(0)$ for the molecule is then given by the following expression:

$$\begin{aligned} ZPE_{r,true} &= G(0) = \frac{1}{2} \sum_r \omega_r + \frac{1}{4} \sum_{r>s} x_{rs} \\ &= \frac{1}{2} \sum_r \omega_r + \frac{1}{4} \sum_r x_{rr} + \frac{1}{4} \sum_{r>s} x_{rs} \end{aligned} \quad (4)$$

The complete set of anharmonicity constants including the diagonal terms x_{rr} and cross-coupling terms x_{rs} is, however, rarely known for most molecular systems and in particular not for transient species as (HCN)₂. We can therefore compare the expression for the “true” vibrational zero-point energy given above with approximate expressions based solely on the sets of either harmonic vibrational energies ω_r or anharmonic vibrational energies ν_r , which are often more accessible. The simplest approximate expression for the vibrational zero-point energy is found when considering solely theoretical harmonic vibrational fundamental energies:

$$ZPE_{harm}^{teo} = \frac{1}{2} \sum_r \omega_r \quad (5)$$

This simple harmonic sum based on the harmonic vibrational energies shown in Table 2 clearly overestimates the “true” vibrational zero-point energy as the difference $ZPE_{true} - ZPE_{harm}^{teo}$ is easily seen to be $\frac{1}{4} \sum_r x_{rr} + \frac{1}{4} \sum_{r>s} x_{rs}$, which in general has a negative value. Alternatively, an approximate expression for the vibrational zero-point energy based on observed (anharmonic) fundamental vibrational band origins can be considered whenever a complete set of fundamental band origins has been explored experimentally. The anharmonic vibrational energy ν_r for the fundamental transition associated with the normal coordinate r is given by:

$$\nu_r = G(\nu_r = 1) - G(\nu_r = 0) = \omega_r + 2x_{rr} + \frac{1}{2} \sum_{r \neq s} x_{rs} \quad (6)$$

The approximate expression for the vibrational zero-point energy based solely on experimental (anharmonic) fundamental band origins will therefore be given by:

$$ZPE_{anh}^{obs} = \frac{1}{2} \sum_r \nu_r = \frac{1}{2} \sum_r \omega_r + \sum_r x_{rr} + \frac{1}{2} \sum_{r>s} x_{rs} \quad (7)$$

This anharmonic sum based on the observed vibrational band origins shown in Table 2 on the other hand underestimates the “true” vibrational zero-point energy as the difference $ZPE_{true} - ZPE_{anh}^{obs}$ is calculated to be $-\frac{3}{4} \sum_r x_{rr} - \frac{1}{4} \sum_{r>s} x_{rs}$, which in general has a positive value. A robust but very simple solution to obtain a much more reliable approximation of the vibrational zero-point energy has been demonstrated by Schaefer III *et al.*^[45] for several simple molecules as H₂O and CH₄, where the complete sets of anharmonicity constants are known experimentally. Schaefer III *et al.* showed that the average value of ZPE_{anh}^{obs} and ZPE_{harm}^{teo} comes very close to the “true” vibrational zero-point energy ZPE_{true} and only slightly underestimate this value with a minor deviation of $-\frac{1}{4} \sum_r x_{rr}$.

The present spectroscopic findings now enable the determination of the total change of vibrational zero-point energy upon dimerization $\Delta ZPE_{total} = \Delta ZPE_{intra} + \Delta ZPE_{inter}$. However, we

first consider the simple approximation based on theoretical harmonic fundamental vibrational energies (eq. 5). The harmonic vibrational zero-point energies of both (HCN)₂ and HCN are combined for the set of intramolecular vibrational fundamental transitions including ν_1 , ν_2 , ν_3 , ν_4 , ν_6^1 and ν_7^1 (the mode numbering for (HCN)₂ given in Table 2) remembering that the ν_6^1 and ν_7^1 fundamentals are both doubly degenerate:

$$\Delta ZPE_{\text{harm,intra}}^{\text{teo}} = \frac{1}{2} \sum_r (\omega_r^{\text{dim}} - \omega_r^{\text{mon}}) \quad (8)$$

The use of previously published harmonic CCSD(T)-F12b/aug-cc-pVQZ intramolecular vibrational fundamental energies for both (HCN)₂ and HCN^[33] then gives $\Delta ZPE_{\text{harm,intra}}^{\text{teo}} = 0.725 \text{ kJ mol}^{-1}$. A harmonic contribution to the vibrational zero-point energy $\Delta ZPE_{\text{harm,inter}}^{\text{teo}}$ from the class of large-amplitude vibrational fundamentals introduced by the complexation including ν_5 , ν_8^1 and ν_9^1 (ν_8^1 and ν_9^1 doubly degenerate) of $2.926 \text{ kJ mol}^{-1}$ comes directly from eq. 5 and provides a total change of vibrational zero-point energy in this simple harmonic approximation $\Delta ZPE_{\text{harm,total}}^{\text{teo}}$ of 3.65 kJ mol^{-1} as listed in Table 3.

Table 3. The total change of vibrational zero-point energy (kJ mol^{-1}) based on theoretical (harmonic) vibrational fundamental energies $\Delta ZPE_{\text{harm}}^{\text{teo}}$ (upper limit) and observed or theoretical anharmonic fundamental energies ΔZPE_{anh} (lower limit). The results are compared to the recent non-empirical benchmark values of D_e and D_0 by Hoobler *et al.*^[38]

	D_e	$\Delta ZPE_{\text{harm}}^{\text{teo}}$	ΔZPE_{anh}	ΔZPE_{best}	D_0
Present work (semi-exp)	19.83 ^[a]	3.65 ^[b]	3.05 ^[c]	3.35 ^[d]	16.48
Hoobler <i>et al.</i> (teo)	19.83 ^[a]		3.03 ^[e]	3.35 ^[f]	16.48

^[a] AE-CCSDT(Q)/CBS value including relativistic and diagonal Born-Oppenheimer terms by Hoobler *et al.*^[37] ^[b] Based on harmonic predictions at the CCSD(T)-F12b/aug-cc-pVQZ level of theory by Mihrin *et al.*^[32] ^[c] Based on observed (anharmonic) fundamental band origins (see text). ^[d] The average value of $\Delta ZPE_{\text{harm}}^{\text{teo}}$ and $\Delta ZPE_{\text{anh}}^{\text{obs}}$ (see text). ^[e] Based on theoretical anharmonic fundamental band origins. ^[f] Second order vibrational perturbation theory (VPT2) at the AE-CCSD(T)/cc-pCVQZ level of theory.

This harmonic approximation for the total change of vibrational zero-point energy upon dimerization clearly overestimates the “true” value as evidenced by Hoobler *et al.*’s non-empirical theoretical prediction of 3.35 kJ mol^{-1} based on second order vibrational perturbation theory at the AE-CCSD(T)/cc-pCVQZ level of theory.^[38]

In our similar approach to obtain the anharmonic change of vibrational zero-point energy $\Delta ZPE_{\text{anh,total}}^{\text{obs}}$ based on the almost complete set of observed fundamental band origins (eq. 7), we first discuss shortly the expected minor contribution from the intramolecular acceptor bending fundamental ν_7^1 , which has not been observed in the gas-phase. The present sensitive long-path FTIR synchrotron spectroscopy approach does not reveal any signs of this transition owing to severe spectral overlaps with monomeric HCN absorption in the vicinity of the degenerate bending fundamental band origin of 711.90 cm^{-1} for HCN. This suggests that the ν_7^1 fundamental transition

indeed is only very slightly blue-shifted relative to the monomer as predicted by both harmonic (dimerization shift of 12 cm^{-1})^[33] and anharmonic (dimerization shift of 11 cm^{-1})^[38] vibrational force field calculations. In general, Hoobler *et al.*’s recent anharmonic predictions reproduce the observed intramolecular complexation shifts rather well with the largest error of 9.15 cm^{-1} for the donor bending fundamental ν_6^1 reported in the present investigation (predicted blue-shift of 58 cm^{-1} versus observed blue-shift of 67.15 cm^{-1}). Assuming a similar maximum relative error for the predicted dimerization shift for the intramolecular acceptor bending ν_7^1 fundamental, we can safely estimate a dimerization blue-shift of $11(2) \text{ cm}^{-1}$ and thereby a band origin of $723(2) \text{ cm}^{-1}$ as given in Table 2.

The approximate anharmonic change of vibrational zero-point energy based on the set of observed fundamental transition energies according to eq. 7 then gives $\Delta ZPE_{\text{anh,intra}}^{\text{obs}} = 0.535 \text{ kJ mol}^{-1}$ and $\Delta ZPE_{\text{anh,inter}}^{\text{obs}} = 2.515 \text{ kJ mol}^{-1}$ and a resulting value for $\Delta ZPE_{\text{anh,total}}^{\text{obs}}$ of 3.05 kJ mol^{-1} as listed in Table 3. This approximate value is a lower limit for the “true” total change of vibrational zero-point energy as argued for above and again indicated by the 0.3 kJ mol^{-1} higher value suggested by Hoobler *et al.*^[37] The best semi-experimental value for the “true” change of vibrational zero-point energy is then achieved by computing the average value of $\Delta ZPE_{\text{harm,total}}^{\text{teo}}$ and $\Delta ZPE_{\text{anh,total}}^{\text{obs}}$ although this average value still underestimates the “true” value slightly. It then appears that our best semi-experimental value matches spot on Hoobler *et al.*’s non-empirical value of 3.35 kJ mol^{-1} (Table 3).

The immediate remarkable correspondence between our semi-experimental value and Hoobler *et al.*’s entirely theoretical value is rather surprising as the application of second order vibrational perturbation theory is known to be notoriously challenging for weakly bound molecular systems. As with any other perturbational approach, one should be careful if the perturbations, the anharmonicity contributions, are of considerable magnitude relative to the zeroth-order harmonic vibrational energy references. The class of large-amplitude intermolecular vibrational modes in particular may be problematic for this kind of perturbational approach, where Hoobler *et al.* reported anharmonicity contributions in the order of 12% and 24% for the ν_8^1 and ν_9^1 fundamentals, respectively. Hoobler *et al.*’s anharmonic analysis showed no Fermi resonance type terms based upon near degeneracy between fundamental transitions and vibrational hot band transitions or strong interactions observed as large cubic force constants. They tested, however, extensively their results by the removal of one or more of the large-amplitude vibrational modes ν_5 , ν_8^1 and ν_9^1 from the anharmonic perturbational treatment. The removal of the ν_8^1 fundamental alone in the anharmonic analysis seemed to produce the most significant effects in the predicted anharmonic band origins, as the ν_9^1 band origin shifts from 35 cm^{-1} to 26 cm^{-1} and the ν_8^1 band origin shifts from 120 cm^{-1} to 136 cm^{-1} .

The complete sets of theoretical anharmonic fundamental band origins for both HCN and (HCN)₂ reported by Hoobler *et al.* enables us to calculate the approximate (lower limit) of the total change of vibrational zero-point energy based on eq. 7

ignoring all involved anharmonicity constants. The extracted value of 3.03 kJ mol^{-1} (Table 3) again is remarkable close to the value based on the complete set of experimental (anharmonic) fundamental band origins of 3.05 kJ mol^{-1} . A closer look at Hoobler *et al.*'s reported non-empirical anharmonic band positions, however, reveals total numeric deviations $\sum_r |v_r^{VPT2} - v_r^{obs}|$ in the order of 10 cm^{-1} for the HCN monomer and 44.7 cm^{-1} for the $(\text{HCN})_2$ system. These deviations would potentially introduce an error of 0.4 kJ mol^{-1} in this approximate value for the total vibrational zero-point energy $\Delta\text{ZPE}_{anh,total}$ if the theoretical anharmonic band origins systematically were predicted at higher energies than the observed band origins. The excellent agreement between the observed and theoretical values of $\Delta\text{ZPE}_{anh,total}$ is partly due to cancellation of errors with opposite signs, where overestimated fundamental band origins are canceled out by underestimated fundamental band positions of the same order of magnitude. Nevertheless, the present semi-experimental approach for the determination of the total change of vibrational zero-point energy upon $(\text{HCN})_2$ complexation combined with the AE-CCSDT(Q)/CBS benchmark D_e -value by Hoobler *et al.* then reproduces the "best" value of $16.48 \text{ kJ mol}^{-1}$ for the dissociation energy D_0 (Table 3). Based on our estimated lower (anharmonic) and higher (harmonic) limits for the "true" value of ΔZPE_{total} , we bracket this final semi-empirical dissociation energy with an error of $\pm 0.30 \text{ kJ mol}^{-1}$, which should even include minor remaining errors of the benchmark electronic energies ($\pm 0.05 \text{ kJ mol}^{-1}$) as suggested by Hoobler *et al.* The present "best" semi-experimental estimate of D_0 is slightly lower than the value of 17.2 kJ mol^{-1} estimated previously by the same authors based on the observed change of vibrational zero-point energy from the class of large-amplitude vibrational modes alone.^[33] The previous semi-experimental estimate of D_0 employed the harmonic prediction of the intramolecular donor bending ν_6^1 fundamental band origin now available by experiment. However, more importantly the present work now employs Schaefer *et al.*'s accurate approach to extract the "true" intermolecular vibrational zero-point energy contribution by considering an average of the theoretical harmonic and experimental (anharmonic) vibrational fundamental energies.^[45]

4. Conclusions

In summary, the generated high-resolution synchrotron infrared absorption spectrum of $(\text{HCN})_2$ has enabled a detailed rovibrational analysis of the missing ν_6^1 band associated with the doubly degenerate donor bending mode. The observed rovibrational structure has the characteristics of a perpendicular type band of a Σ -II transition for a linear polyatomic molecule and in total 100 spectral lines belonging to the P-, Q-, and R-branches have been assigned and fitted simultaneously to a standard semi-rigid linear molecule Hamiltonian. The resulting fit provides an accurate value for the missing band origin ν_0 of $779.05182(50) \text{ cm}^{-1}$ together with the spectroscopic parameters B' , D' , and q for the doubly degenerate excited state ν_6^1 . This accurate ν_6^1 fundamental band origin, blue-shifted by

67.15 cm^{-1} relative to the degenerate HCN monomer bending band origin, provides the final significant contribution of 0.8 kJ mol^{-1} to the change of *intra*-molecular vibrational zero-point energy upon complexation and the best semi-experimental estimate of $3.35 \pm 0.30 \text{ kJ mol}^{-1}$ for the total change of vibrational zero-point energy. The combination with Hoobler *et al.*'s^[37] AE-CCSDT(Q)/CBS benchmark value for the interaction energy D_e of $19.83 \text{ kJ mol}^{-1}$ including relativistic and diagonal Born-Oppenheimer corrections then enables a reliable semi-experimental value of $16.48 \pm 0.30 \text{ kJ mol}^{-1}$ for the intermolecular hydrogen bond energy D_0 .

Supporting Information

The observed and calculated line positions from the rovibrational analysis of the ν_6^1 band are given as electronic supporting information.

Acknowledgements

RWL acknowledges Synchrotron SOLEIL for the granted beam-time for proposal 20170820. RWL and AV acknowledge financial support by the CALIPSOplus project funded by the European Union's Horizon 2020 Research and Innovation programme. The authors finally thank the SOLEIL chemistry laboratory support team led by S. Blanchandin for their valuable assistance and M. A. Sánchez for help during the measurements.

Conflict of Interest

The authors declare no conflict of interest.

Keywords: Dissociation Energy · Hydrogen Bonding · Infrared Synchrotron Radiation · Non-Covalent Forces · Vibrational Zero-Point Energy

- [1] E. J. Bohac, M. D. Marshall, R. E. Miller, *J. Chem. Phys.* **1992**, *96*, 6681.
- [2] J. Rezac, P. Hobza, *J. Chem. Theory Comput.* **2014**, *10*, 3066–3073.
- [3] B. E. Rocher-Casterline, L. C. Ch'ng, A. K. Mollner, H. Reisler, *J. Chem. Phys.* **2011**, *134*, 211101.
- [4] A. Shank, Y. Wang, A. Kaledin, B. J. Braams, J. M. Bowman, *J. Chem. Phys.* **2000**, *130*, 144314.
- [5] G. S. Tschumper, M. L. Leininger, B. C. Hoffman, E. F. Valeev, H. F. Schaefer, M. Quack, *J. Chem. Phys.* **2002**, *116*, 690–701.
- [6] F. Kollipost, R. Wugt Larsen, A. V. Domanskaya, M. Noerenberg, M. A. Suhm, *J. Chem. Phys.* **2012**, *136*.
- [7] Z. Xu, M. A. Suhm, *J. Chem. Phys.* **2009**, *131*, 054301.
- [8] A. C. Legon, D. J. Millen, P. J. Mjoberg, *Chem. Phys. Lett.* **1977**, *47*, 589–591.
- [9] R. D. Brown, P. D. Godfrey, D. A. Winkler, *J. Mol. Spectrosc.* **1981**, *89*, 352–355.
- [10] R. Wugt Larsen, F. Pawlowski, F. Hegelund, P. Jørgensen, J. Gauss, B. Nelander, *Phys. Chem. Chem. Phys.* **2003**, *5*, 5031–5037.
- [11] L. W. Buxton, E. J. Campbell, W. H. Flygare, *Chem. Phys.* **1981**, *56*, 399–406.
- [12] A. J. Fillery-Travis, A. C. Legon, L. C. Willoughby, A. D. Buckingham, *Chem. Phys. Lett.* **1981**, *102*, 126–131.
- [13] E. J. Campbell, S. G. Kukolich, *Chem. Phys.* **1983**, *76*, 225–229.

- [14] K. Georgiou, A. C. Legon, D. J. Millen, P. J. Mjöberg, *Proc. R. Soc. London Ser. A* **1985**, *399*, 377–390.
- [15] R. S. Ruoff, T. Emilsson, C. Chuang, T. D. Klots, H. S. Gutowsky, *Chem. Phys. Lett.* **1987**, *138*, 553–558.
- [16] A. Haynes, A. C. Legon, *J. Mol. Struct.* **1988**, *189*, 153–164.
- [17] R. E. Bumgarner, G. A. Blake, *Chem. Phys. Lett.* **1989**, *161*, 308–314.
- [18] B. A. Wofford, J. W. Bevan, W. B. Olson, W. J. Lafferty, *J. Chem. Phys.* **1986**, *85*, 105–108.
- [19] K. W. Jucks, R. E. Miller, *J. Chem. Phys.* **1988**, *88*, 6059–6067.
- [20] K. W. Jucks, R. E. Miller, *Chem. Phys. Lett.* **1988**, *147*, 137–141.
- [21] D. S. Anex, E. R. Davidson, C. Douketis, G. E. Ewing, *J. Phys. Chem.* **1988**, *92*, 2913–2925.
- [22] J. Meyer, E. R. T. H. Kerstel, D. Zhuang, G. Scoles, *J. Chem. Phys.* **1989**, *90*, 4623–4625.
- [23] E. R. T. H. Kerstel, K. K. Lehmann, J. E. Gambogi, X. Yang, G. J. Scoles, *Chem. Phys.* **1993**, *99*, 8559–8570.
- [24] R. Wugt Larsen, F. Hegelund, B. Nelander, *Phys. Chem. Chem. Phys.* **2004**, *6*, 3077–3080.
- [25] G. A. Hopkins, M. Maroncelli, J. W. Nibler, *Chem. Phys. Lett.* **1985**, *114*, 97–102.
- [26] M. Maroncelli, G. A. Hopkins, J. W. Nibler, T. R. Dyke, *J. Chem. Phys.* **1985**, *83*, 2129–2146.
- [27] A. Grushow, W. A. Burns, K. R. Leopold, *J. Mol. Spectrosc.* **1995**, *170*, 335–345.
- [28] J. Andersen, J. Heimdal, B. Nelander, R. Wugt Larsen, *J. Chem. Phys.* **2017**, *146*, 194302.
- [29] J. Andersen, J. Heimdal, R. Wugt Larsen, *Phys. Chem. Chem. Phys.* **2015**, *17*, 23761–23769.
- [30] J. Andersen, J. Heimdal, R. Wugt Larsen, *J. Chem. Phys.* **2015**, *143*, 224315.
- [31] F. Kollipost, J. Andersen, D. Mahler, J. Heimdal, M. Heger, M. A. Suhm, R. Wugt Larsen, *J. Chem. Phys.* **2014**, *141*, 174314.
- [32] J. Andersen, J. Heimdal, D. W. Mahler, B. Nelander, R. W. Larsen, *J. Chem. Phys.* **2014**, *140*, 091103.
- [33] D. Mihin, P. W. Jakobsen, A. Voute, L. Manceron, R. Wugt Larsen, *Phys. Chem. Chem. Phys.* **2018**, *20*, 8241–8246.
- [34] R. Wugt Larsen, F. Hegelund, B. Nelander, *J. Phys. Chem. A* **2004**, *108*, 1524–1530.
- [35] R. Wugt Larsen, F. Hegelund, B. Nelander, *Phys. Chem. Chem. Phys.* **2005**, *7*, 1953–1959.
- [36] R. Wugt Larsen, F. Hegelund, B. Nelander, *J. Phys. Chem. A* **2005**, *109*, 4459–4463.
- [37] R. Wugt Larsen, F. Hegelund, B. Nelander, *Mol. Phys.* **2004**, *102*, 1743–1748.
- [38] P. R. Hoobler, J. M. Turney, J. Agarwal, H. F. Schaefer III, *ChemPhysChem* **2018**, *19*, 3257–3265.
- [39] F. Kwabia Tchana, F. Willaert, X. Landsheere, J.-M. Flaud, L. Lago, M. Chapuis, P. Roy, L. Manceron, *Rev. Sci. Instrum.* **2013**, *84*, 093101.
- [40] S. M. Chernin, E. G. Barskaya, *Appl. Opt.* **1991**, *30*, 51–58.
- [41] A. R. W. Mckellar, *J. Mol. Spectrosc.* **2010**, *262*, 1–10.
- [42] M. Faye, M. Bordessoule, B. Kanouté, J.-B. Brubach, P. Roy, L. Manceron, *Rev. Sci. Instrum.* **2016**, *87*, 063119.
- [43] V.-M. Horneman, *J. Mol. Spectrosc.* **2007**, *241*, 45–50.
- [44] C. M. Western, B. E. Billinghurst, *Phys. Chem. Chem. Phys.* **2017**, *19*, 10222–10226.
- [45] R. S. Grev, C. L. Janssen, H. F. Schaefer III, *J. Chem. Phys.* **1995**, *95*, 5128–5132.

Manuscript received: August 14, 2019
Version of record online: November 8, 2019